NORTHWESTERN
UNIVERSITY

Center for Sustainable Engineering of Geological and Infrastructure Materials

Department of Civil and Environmental Engineering

McCormick School of Engineering and Applied Science

Evanston, Illinois 60208, USA

Experimental Characterization of Marcellus Shale

Gianluca Cusatis, Congrui Jin, & Weixin Li

SEGIM INTERNAL REPORT No. 15-08/478E

Abstract

Experimental methods are the most important and reliable way to study rock properties and rock failure mechanisms. The failure mechanism of rock materials due to their mineralogical texture is complex and it is more problematic for anisotropic rock. In this study, seismic velocity measurement, Brazilian tensile strength test, uniaxial (unconfined) compressive strength test, and three point bending test, are conducted on shale specimens to study their properties. The shale used in this study was taken from a Marcellus Shale outcrop in Pennsylvania. For the purpose of comparison, some tests were also conducted on grey shale specimens, taken from Thornton Quarry, located in Thornton, Illinois, just south of Chicago. The results are also compared with the experimental data on Boryeong shale obtained from existing literature. In this study, the experimental results of seismic properties, strength properties and fracture behavior of Marcellus shale specimens have been reported and discussed in great details.

Keywords: Shale, Fracture, Strength, Experiments

1. Introduction

Tight and shale gas are emerging as a potentially key component of the worldwide energy landscape and it is affecting US energy independence with reserves projected to last for many decades to come and probably over a century. Accompanying the resource potential of gas shale is a new interest in understanding the geological, physical, and mechanical properties of shale. One of the most urgent technical challenges for the development of unconventional shale gas in the foreseeable future is the integration of computational modeling techniques and novel experimental methods. In other words, formulation and validation of computational models should incorporate a rich set of experimental data, reproducing not only the global stress-strain response, but also the patterns of damage and localized deformation emerging during loading. This task requires a comprehensive database of shale characteristics and its mechanical properties at various length scales. Unfortunately, it has previously been assumed that shale was not a reservoir rock, and thus not

interesting in terms of hydrocarbon production, which has led to a lack of published experimental data on shale samples.

The key goal of our work is to perform a thorough experimental campaign to collect data at multiple length scales from gas shale samples, especially from Marcellus black shale samples, as shown in Fig. 1. We report a systematic analysis on the anisotropic behaviors in strength and fracture patterns observed during Brazilian tests and compression tests on Marcellus black shale samples. We present comprehensive data on the general mechanical behavior of Marcellus shale samples, the static and dynamic elastic properties, and the variations of uniaxial and tensile strength as functions of the anisotropy angle with respect to the lamination. Three point bending tests are also performed to study the failure mechanisms of shale. For the purpose of comparison, some tests were also conducted on grey shale specimens, taken from Thornton Quarry, located in Thornton, Illinois, just south of Chicago. The results are also compared with the experimental data on Boryeong shale obtained from existing literature [1, 2].

2. Experimental Methods

2.1. Sample Preparation

Shale is often considered as a type of transversely isotropic rock material, i.e. rocks with one dominant direction of planar anisotropy. Marcellus shale shows heterogeneity at micro-scale (i.e. at the mineral scale). But at macro-scale, they also show a clear evidence of transverse isotropy due to the partial alignment of anisotropic clay minerals, as observed in Fig. 1. The tested samples have an average mass density of 2558 kg/m^3. The specimens were free of surface cracks and voids. Prior to testing, all the specimens were ground and polished by hand. The hand-grinding was done to avoid disturbances from machining during the sample preparation. Three types of specimens were prepared for further tests.

The first type is cube specimens with a nominal dimension of 1 in $\times$ 1 in $\times$ 1 in. Cube specimens were cut by a band saw, as shown in Fig. 2, from a large shale block in such a way that the bedding plane direction and the cube edge has a angle, called anisotropy angle, denoted by the angle θ, which is measured clockwise from the loading direction relative to the bedding plane, as shown in Fig. 3. The anisotropy angle θ varied between 0° (perpendicular to the loading direction) and 90° (parallel to the loading direction). Bedding direction was marked by solid lines after cutting. Specimens with 5 different

anisotropy angles of 0°, 30°, 45°, 60° and 90° were prepared and shown in Fig. 4. These cube specimens were used for seismic velocity measurement, Brazilian tensile test and uniaxial compression test.

The second type is disc specimens with a nominal diameter, D, of 38 mm and a nominal height, t, of 19 mm. The laboratory directional coring system, as shown in Fig. 2, was used to obtain the disc samples. The shale block was properly clamped to prevent any unwanted movement during the coring process. The speed of coring was constant to avoid any irregularities or defects on the cutting surface. The specimens were cored along the bedding plane. These specimens were used for Brazilian tensile tests. Different anisotropy angles were achieved by simply rotating the disk during the tests.

The third type is notched beam specimens. The nominal dimensions of the length L, width W, and thickness B of the specimens are 100 mm, 25 mm and 12.5 mm, respectively. The dimensions of the specimen are provided such that they compile with ASTM requirements. The width of the specimen is controlled by the length, i.e., length to width ratio should be approximately equal to 4. The value of the specimen thickness B should be varied from $0.25W$ to W. The band saw was used to cut a notch of length $a = 6$ mm for each specimen. We prepared three types of notched beam specimens for different bedding plane orientations, as shown in Fig. 5. These specimens were used for three point bending tests.

2.2. Seismic Velocity Measurement

A seismic velocity measurement system was used to determine the longitudinal elastic wave (P-wave) velocity of Marcellus shale samples, as shown in Fig. 6. The ultrasonic system consists of several functional units, such as the pulser/receiver, transducer, and a display device. A pulser/receiver is an electronic device that can produce high voltage electrical pulses. Driven by the pulser, the transducer generates high frequency ultrasonic energy. The sound energy is introduced and propagates through the materials in the form of stress waves. The wave signal is transformed into an electrical signal by the transducer and is displayed on a screen. The velocity of the wave is calculated as the distance that the signal traveled divided by the travel time.

2.3. Brazilian Tensile Strength Test

The Brazilian test is a simple indirect testing method to obtain the tensile strength of brittle and quasi-brittle material such as concrete, rock, and rock-like materials. In this study, the Brazilian tests were conducted on both

Marcellus black shale specimens and grey shale specimens. The tests were conducted at the 1000 kips MTS loading system operated in a stroke mode, as shown in Fig. 7. The MTS loading system consists of a main frame, a hydraulic pump unit, a controller, a load cell and a computer. Specimens were loaded up to failure at a constant displacement rate of 0.003 mm/s. The loading configuration, as shown in Fig. 7, was used in the experiment. For cube specimens, wood strips were used as cushion. After the failure of specimens, pieces of failed rock specimens were collected to investigate the relationship between the bedding plane and the failure plane.

The indirect tensile strength, perpendicular to the loaded diameter, based on linear elastic calculations for homogeneous and isotropic rock is written as $\sigma_t = 2kP/(Dt)$, where P is the load at failure, D is the diameter of the test specimen (or the edge length of the cube specimen), t is the thickness of the test specimen measured at the center, and k is a coefficient depending on the specimen geometry and experimental conditions. For disc tests, $k = 1/\pi$, and $k \approx 0.3$ for cube tests [3]. Of course this formula is considered for the loaded diameter in the condition of a typical vertical splitting, which is often not the case for transversally isotropic rock material. Therefore, this formula is used just for comparison purposes and the results do not necessarily present the tensile strength of the samples [4].

2.4. Uniaxial Compressive Strength Test

Cube specimens were loaded up to failure at a constant displacement rate of 0.001 mm/s using the same 1000 kips MTS loading system as the one used in Brazilian tensile strength test. Specimens were placed between two loading platens, as shown in Fig. 8. The tests were carried out with specimen and steel loading platens in direct contact with each other, and Dry Moly Lube was sprayed between the steel platens and specimens to reduce friction. After the failure of specimens, pieces of failed specimens were collected to investigate the relationship between the bedding plane and the failure plane. The uniaxial compressive strength (UCS) was approximated by the maximum nominal stress, i.e., $\sigma_c = F/A$, where F is the peak load, and A is the initial area of specimen cross section.

2.5. Three Point Bending Test

This method covers the determination of the plane-strain fracture toughness of shale using a three-point bending test on a single-edge notched beam specimen. These plane-strain fracture toughness results will be applicable

whenever there is a fracture involved in operation, e.g., in the resource recovery process such as stimulation of oil and gas wells by hydraulic fracturing, fragmentation of oil shale beds for in-situ retorting, and stress induced fracturing of geothermal sources. In this study, three point bending tests were conducted on both Marcellus black shale specimens and grey shale specimens.

Notched beams were placed on the three point bending fixture with a nominal span $S = 75$ mm, as shown in Fig. 9. The experimental setup consists of two parallel supports for the sample and a single loading pin in the middle, between the supports, where the force is introduced. The support pins must be mounted in such a way that they can rotate freely on their axes in order to minimize the influence of friction on the measurement. One of the supports must also be able to rotate about an axis perpendicular to this and parallel to the axes of the sample so that the test piece can align itself when under stress. The loading pin must also possess similar rotational axes in order to ensure the uniform application of force on the test piece. The crack growth is monitored by measuring crack opening displacement with an extensometer mounted, as shown in Fig. 9. The samples are loaded using a 20 kips MTS loading system. The rate of loading is controlled by the notch opening displacement, and the crack mouth opening rate for all the tests is 0.0005 mm/s. The specimens are tested for three different orientations.

The stress intensity factor, K_{IC}, can be calculated using Griffith's relationship as: $K_{IC} = 6Ma^{1/2}F(a/W)/(BW^2)$, where $F(a/W)$ is a correction factor [5], $M = P_C S/4$ is the applied bending moment, a is notch length, B is thickness of the specimen, W is depth of the specimen, S is span length, and P_C is peak load. This equation is valid for a/W between zero and 0.6.

3. Results and Discussion

3.1. Variation of P-Wave Velocity with Anisotropy Angle

Fig. 10 shows the variation of the P-wave velocity with respect to the anisotropy angle for Marcellus shale. For the purpose of comparison, we also presented the experimental results on Boryeong shale obtained from existing literature [2]. It indicates that in general, the variations of P-wave velocity with anisotropy angle of Boryeong shale and Marcellus shale show similar trends. The maximum values occurred in the direction parallel to the isotropic plane, and the minimum value occurred in the direction perpendicular to the isotropic plane. In the case of Boryeong shale, the P-wave

velocity varies from 3520 m/s to 5140 m/s, while the measured P-wave velocity for Marcellus shale varies from 3104 m/s to 5481 m/s. The maximum and the minimum P-wave velocities both occurred at the anisotropy angles of 90° and0°, respectively. The anisotropy ratios of P-wave velocity, defined as V_P^{max}/V_P^{min} are about 1.8 and 1.5 for Marcellus shale and Boryeong shale, respectively.

3.2. Tensile Strength Anisotropy

The results of Brazilian tests on Marcellus shale are presented in Table 1 and Fig. 11. In Table 1, for disc tests $k = 0.318$; and $k = 0.307$ for cube tests. Note that the formula to calculate σ_t is inaccurate when the thickness of the specimen is significant [6], but the size correction factor is ignored in Table 1. From Fig. 11 and Table 1, it can be seen that the maximum tensile strength occurred at or near $\theta = 0°$, while the minimum value occurred at $\theta = 90°$. Fig. 11 implies that Boryeong shale and Marcellus shale show similar trends of the variation of tensile strength with anisotropy angle: the tensile strength increases slightly from 0° to 45°, followed by a decrease from 45° to 90°. The anisotropy ratio calculated by $\sigma_c^{max}/\sigma_c^{min}$ is about 1.6 for Marcellus shale, which is smaller than 2.1, the ratio for Boryeong shale. This may by explained by the fact that bedding layers in Marcellus shale are more rigidly consolidated. The shale specimens are observed to fail suddenly during the tests, demonstrating that the material is brittle. By studying the shale samples after failure, we observed that, in almost all the samples, the crack propagates along the loaded diameter, as shown in Fig. 12.

For the purpose of comparison, some tests were also conducted on grey shale core specimens. For the experiments conducted on disc specimens, the loading direction is always perpendicular to the bedding; and for cube specimens, the loading direction is either perpendicular or parallel to the bedding, as shown in Fig. 13(a). In sharp contrast, for grey shale specimens, two different types of fractures are observed, as shown in Fig. 13(b): (A) one propagates along the loaded diameter; and (B) the other fails along the bedding layers. The results of Brazilian tests on grey shale are presented in Table 2. The grey shale specimens after failure are shown in Fig. 14. It can be seen that the specimens show a failure by either Mode A only or a combination of both Mode A and Mode B. The rupture of a chain occurs at the weakest link. It is a law of nature that a fracture grows and propagates along a path and direction that needs less energy to dissipate. In a layered rock, the boundaries of the bedding layers are considered as the

planes of weakness. When mentioned planes are frequent, it is logical that fractures use one or more of them to propagate. It has been observed that the bedding layer boundaries' frequency and weak mineral (mica and carbonate) percentage are directly proportional to each other [7]. More weak minerals cause layer activation, becoming more dominant in the fracture pattern. For larger weak minerals percentage, a decrease of the tensile strength is reported [7]. This is consistent with the results presented in Table 2, which shows that when Mode A and Mode B happen simultaneously, the values of tensile strength are considerably lower. In the case of $\theta = 90°B$, if a straight fracture parallel to the bedding layers between both loading platens is induced, it is classified as layer activation; however, if the fracture locates in the central part but does not follow the bedding layer, it is classified as vertical central splitting. Without a microscope it is not possible to judge in which mode the specimen fails in this case, but since the direction of plane of weakness and loading axis are very close to each other, Mode B should function in most of the cases, i.e., fractures grow through bedding layers in order to dissipate less energy.

Similar to the results on grey shale, the experimental results on Boryeong shale also demonstrates that although tensile splitting is the dominant failure mode for most of cases, the shear failure along the bedding layers occurred simultaneously [1].

3.3. Uniaxial Compressive Strength Anisotropy

The results of uniaxial compression tests on Marcellus shale are presented in Table 3 and Fig. 15. Compared to the results of Boryeong shale, the compression strength of Marcellus shale is lower. The compression strength of Boryeong shale varies from 62 to 144 MPa, while it varies from 26 to 99 MPa for Marcellus shale. However, the general trends of the variation of compression strength for Marcellus shale and Boryeong shale are quite similar. The maximum uniaxial compressive strength occurs at $\theta = 0°$ or $\theta = 90°$, and they exhibit minimum strength at approximately $45° < \theta < 75°$. The anisotropy ratio of uniaxial compressive strength, calculated by $\sigma_c^{max}/\sigma_c^{min}$, is about 3.2 for Marcellus shale, which is a little larger than 2.6, the ratio for Boryeong shale.

The variation of uniaxial compressive strength can be explained by the effect of weakness plane, i.e. when the failure plane coincides with the weakness plane, failure occurs at a lower stress level. This is due to the fact that shear cracks develop more easily along the weakness plane. The bedding

layers can be assumed as the weakness planes. Fig. 16 shows the specimens after uniaxial compression failure. The specimens mostly failed along the bedding layers when $45° < \theta < 90°$.

3.4. Three Point Bending Test Results

The results for three point bending tests for Marcellus shale are tabulated in Table 4. The load-displacement curves are linear up to peak. We were not able to capture the post-peak behavior for Marcellus shale specimens, probably because Marcellus shale is very brittle. In sharp contrast, for grey shale specimens, we were able to capture the post-peak behavior through steady crack propagation for all the samples, but the results for grey shale will not be discussed here. Table 4 shows that the specimen with the bedding layer parallel to the loading direction exhibits lower K_{IC} than the other two specimens with the bedding plane perpendicular to the loading direction. The anisotropy ratio of K_{IC} calculated by $K_{IC}^{max}/K_{IC}^{min}$ is about 1.3. The fracture leaves a relatively flat at surface at the break, as shown in Fig. 17.

4. Conclusions

This study provides the results of experimental investigation of the anisotropy of strength, P-wave velocities and fracture properties for Marcellus shale. The experimental results of Marcellus shale were compared with grey shale and Boryeong shale. The anisotropy ratios of P-wave velocities, Brazailian tensile strength, uniaxial compressive strength, and critical stress intensity factor were obtained and discussed. The following conclusions can be made.

1. The variations of P-wave velocity of Marcellus shale and Boryeong shale show similar trends with anisotropy angle. The maximum values occurred in the direction parallel to bedding plane, and the minimum value occurred in the direction perpendicular to bedding plane. The measured P-wave velocities for Marcellus shale vary from 3104 m/s to 5481 m/s. The maximum and minimum P-wave velocities occurred at the anisotropy angles of 90° and 0°, respectively.
2. The Brazilian tensile strength of Marcellus shale is generally lower than that of Boryeong shale, but they share the same trend of the variation of tensile strength with anisotropy angle, which exhibit an increase of strength between 0° and about 45° followed by a decrease. For Marcellus shale, the crack generally propagates along the loading direction for almost all the specimens.

3. The uniaxial compressive strength of Marcellus shale is also lower than that of Boryeong shale. The minimum strength occurs at approximately $45° \leq \theta \leq 75°$. The specimens mostly failed along the bedding layers when $30° \leq \theta \leq 90°$.

Acknowledgement

We would like to thank Professor Sageman from Department of Earth & Planetary Sciences for providing the Marcellus black shale samples.

References

[1] Jung-Woo Cho, Hanna Kim, Seokwon Jeon, and Ki-Bok Min. Deformation and strength anisotropy of asan gneiss, boryeong shale, and yeoncheon schist. 50, 158-169.

[2] Hanna Kim, Jung-Woo Cho, Insun Song, and Ki-Bok Min. Anisotropy of elastic moduli, p-wave velocities, and thermal conductivities of asan gneiss, boryeong shale, and yeoncheon schist in korea. 147148, 68-77.

[3] Rock Failure Mechanisms: Illustrated and Explained. Chun'An Tang, John A. Hudson. CRC Press, 2010.

[4] A. Tavallali, A. Vervoort, Effect of layer orientation on the failure of layered sandstone under Brazilian test conditions, International Journal of Rock Mechanics and Mining Sciences, 47 (2010), 313-322.

[5] Zdenek P. Bazant and Jaime Planas. Fracture and Size Effect in Concrete and Other Quasibrittle Materials. CRC Press.

[6] Yu, Y., Yin, J., Zhong, Z., Shape effects in the Brazilian tensile strength test and a 3D FEM correction. Int. J. Rock Mech. Min. Sci., 43:623-627, 2006.

[7] A. Tavallali, A. Vervoort, Failure of layered sandstone under Brazilian test conditions: effect of micro-scale parameters on macro-scale behavior Rock Mechanics and Rock Engineering, 2010, 43, 641-653.

Table 1: Brazilian Test Results on Marcellus Shale Specimens

θ [°]	Specimen Type	σ_t [MPa]				Mean [MPa]
0	Disc	6.18	4.60	5.42	4.03	5.06
10	Disc	5.22	5.28	4.60	5.28	5.10
25	Disc	7.25	5.93	5.10	7.11	6.35
45	Disc	4.66	5.26	6.31	4.70	5.23
60	Disc	5.53	5.74	5.48	6.41	5.79
80	Disc	5.26	4.29	6.10	4.98	5.16
90	Disc	3.83	3.75	3.66	3.77	3.75
0	Cube	10.22	10.30	9.37	9.70	9.90
90	Cube	4.31	3.95	5.13	4.74	4.53

Table 2: Brazilian Test Results on Grey Shale Specimens

θ [°]	Specimen Type	Failure Mode	σ_t [MPa]				Mean [MPa]
90	Disc	A & B	9.91	6.32	7.51	7.83	7.89
90	Disc	A	9.20	13.71	12.22	12.54	11.92
0	Cube	A & B	8.25	6.59	9.69	7.01	7.89
0	Cube	A	11.66	10.16	12.17	11.39	11.35
90A	Cube	A & B	6.53	4.22	3.14	3.41	4.33
90A	Cube	A	9.86	13.82	12.61	10.98	11.82
90B	Cube	A or B	7.28	5.12	7.91	6.07	6.60

Table 3: Uniaxial Compression Test Results on Marcellus Shale Specimens

θ [°]	Specimen Type	σ_c [MPa]			Mean [MPa]
0	Cube	84.31	81.90	blank	blank
30	Cube	51.91	38.59	blank	blank
45	Cube	26.37	30.72	blank	blank
60	Cube	66.95	30.42	blank	blank
90	Cube	98.99	50.53	blank	blank

Table 4: Three Point Bending Test Results on Marcellus Shale Specimens

Bedding Layer Orientation	Peak Load [N]	K_{IC} (MPa$\sqrt{m}$)
x-y	678	1.34
x-z	533	1.06
y-z	622	1.23

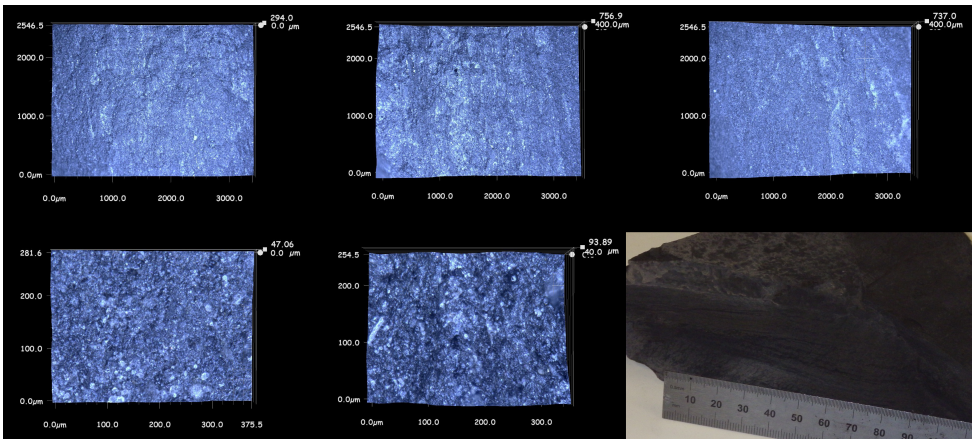

Figure 1: Photos and micrographs of several representative samples used in the experiments. All the micrographs are oriented with the bedding direction from top to bottom.

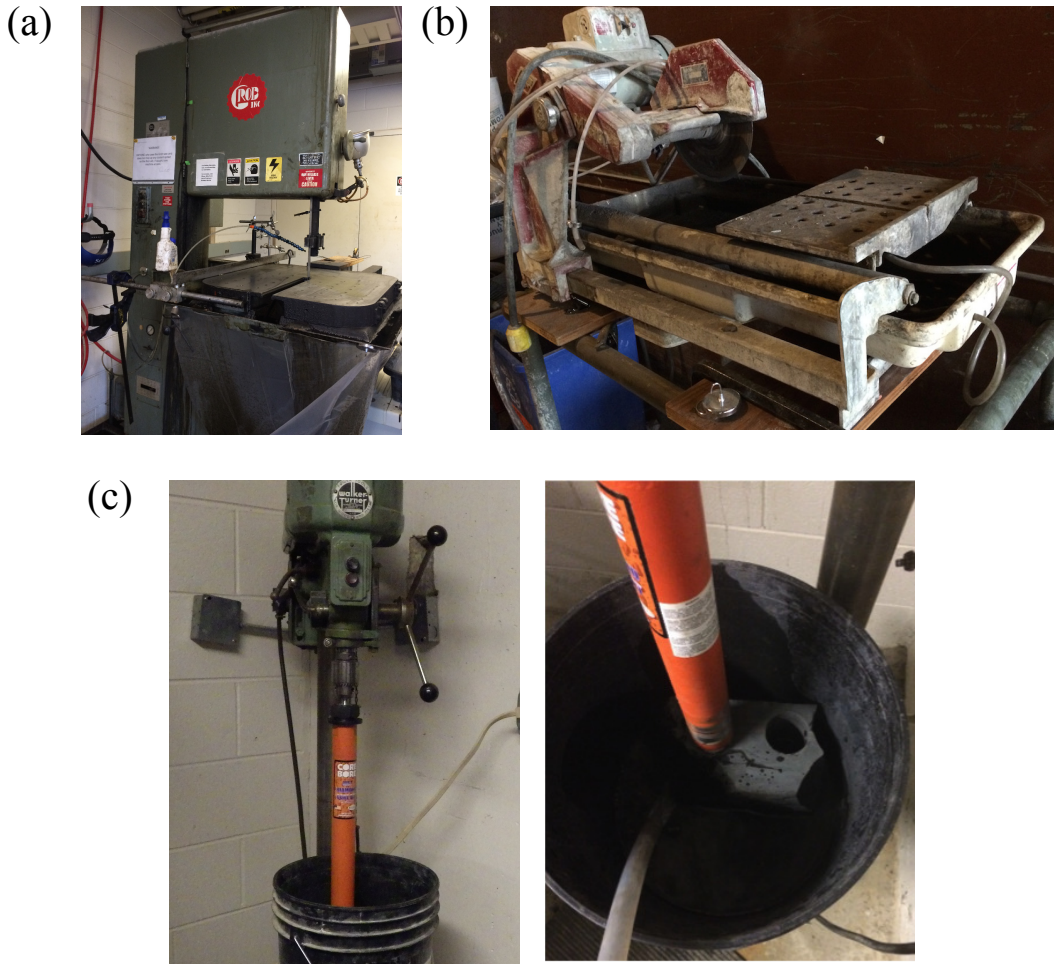

Figure 2: Sample preparation tools: (a) Band saw for cutting cube sample; (b) Circular saw for cutting large blocks into small pieces; (c) Directional coring for disc sample preparation.

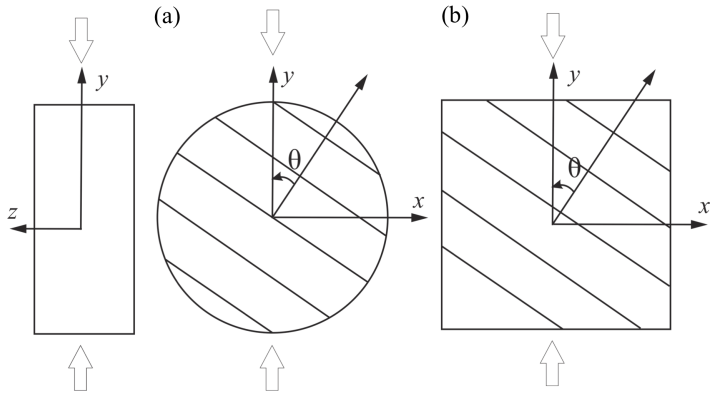

Figure 3: Definition of anisotropy angle: (a) Disc specimen; (b) Cube specimen.

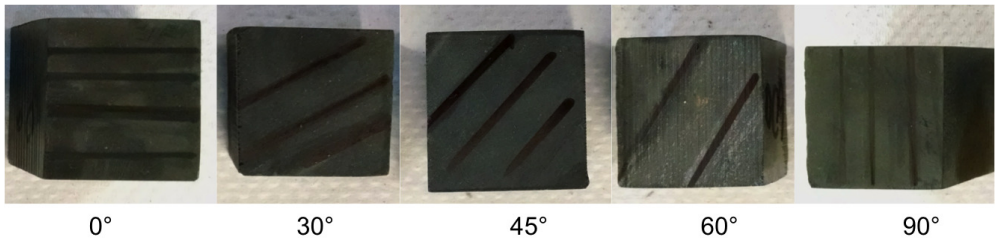

Figure 4: Specimens with 5 different anisotropy angles of 0°, 30°, 45°, 60° and 90° were prepared.

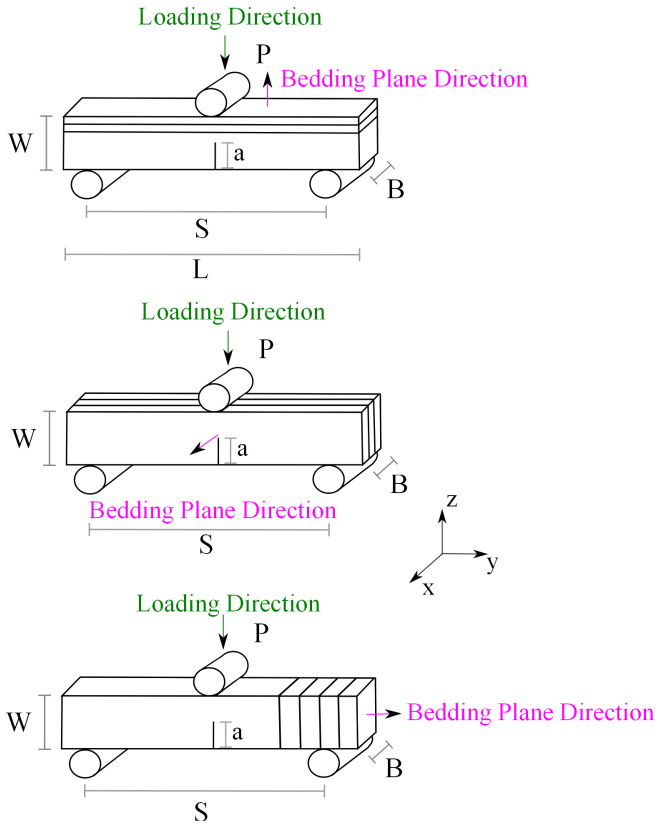

Figure 5: Three types of notched beam specimens for different bedding plane orientations: specimens with bedding plane parallel to x-y plane; specimens with bedding plane parallel to x-z plane; and specimens with bedding plane parallel to y-z plane.

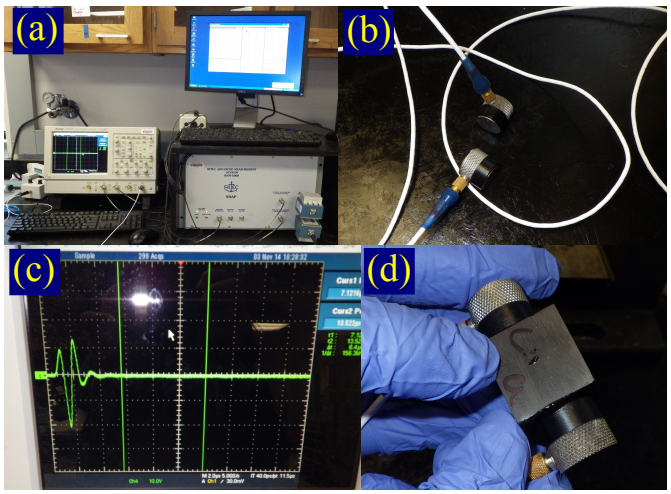

Figure 6: The measurement system used to determine the P-wave velocity of each sample. (a) RAM-5000 computer controlled ultrasonic system; (b) Transmitter and receiver; (c) Oscilloscope; and (d) Experimental sample.

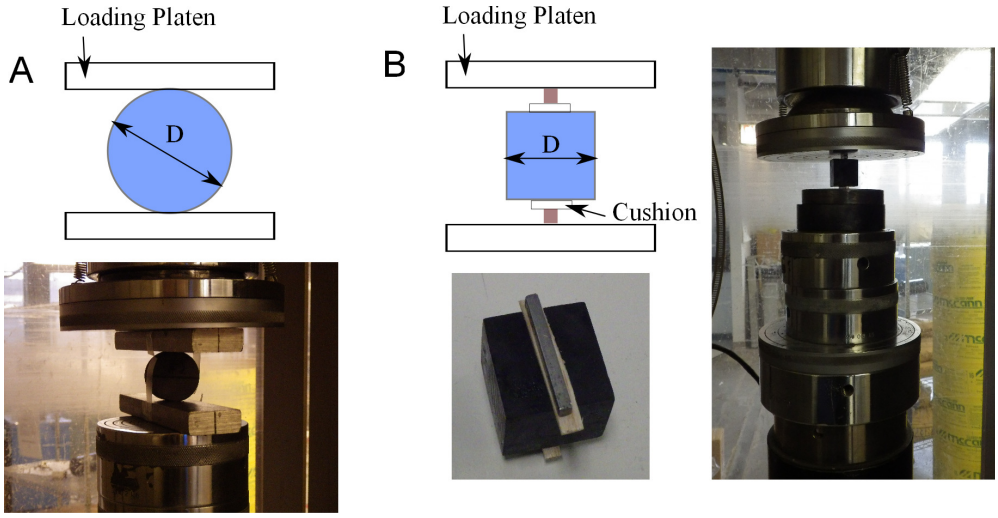

Figure 7: Loading configuration used in Brazilian test: (a) Disc specimen; (b) Cube specimen.

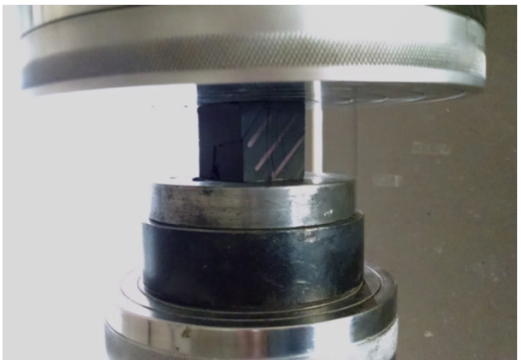

Figure 8: Loading configuration used in uniaxial compression test.

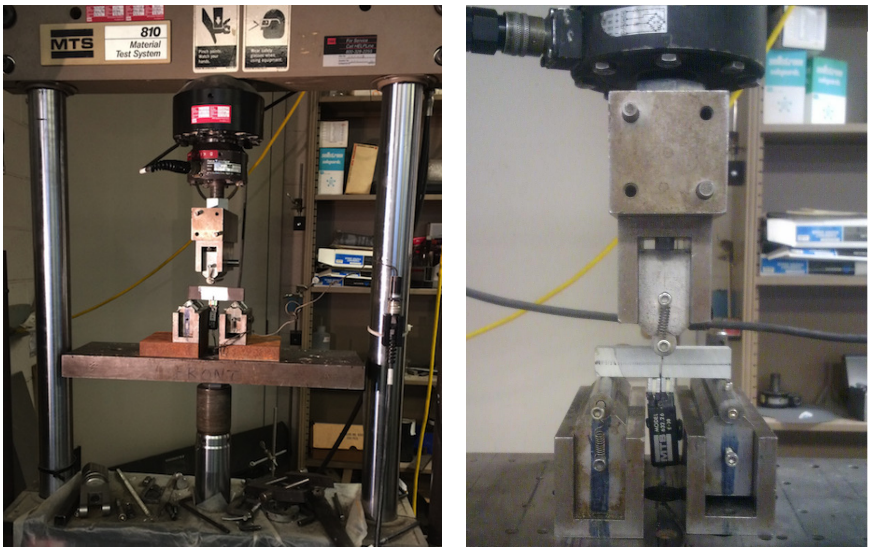

Figure 9: Loading configuration used in three point bending test.

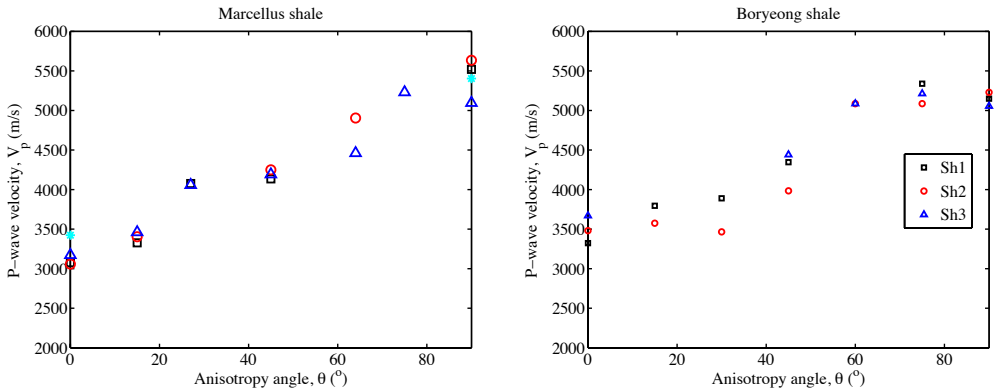

Figure 10: P-wave velocity variation with respect to anisotropy angle: (a) Marcellus shale; (b) Boryeong shale.

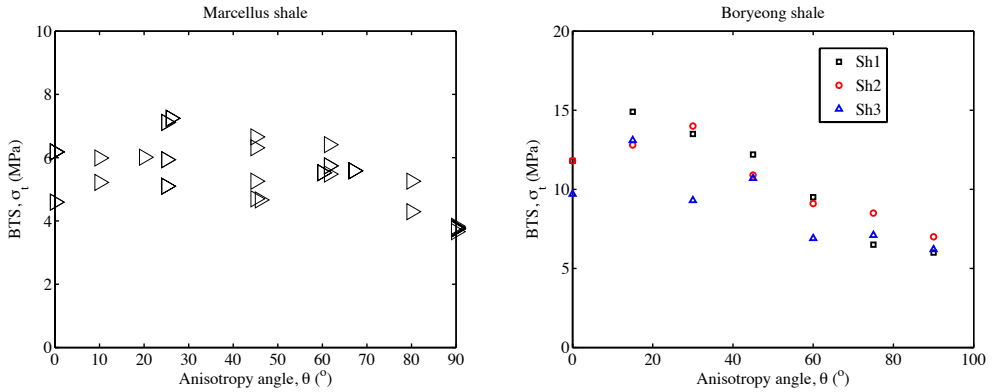

Figure 11: Tesile strength variation with respect to anisotropy angle: (a) Marcellus shale; (b) Boryeong shale.

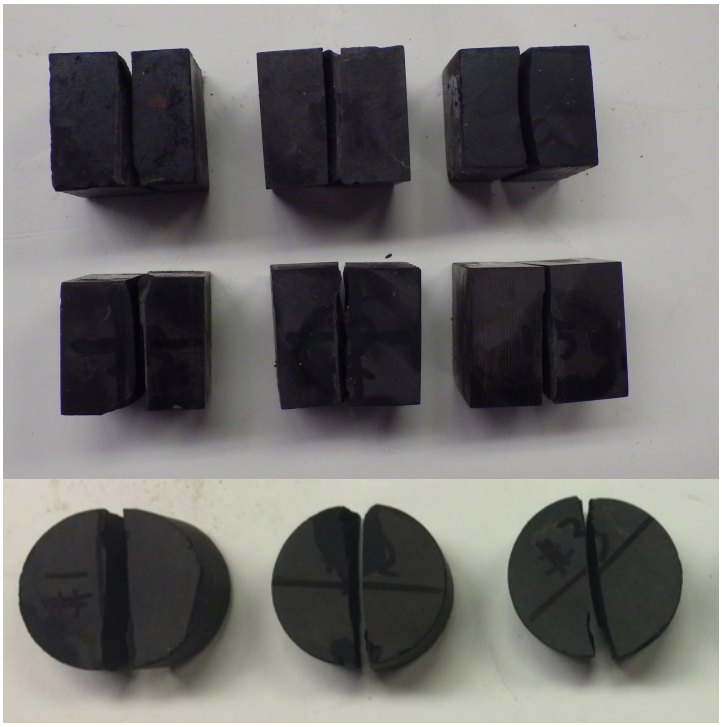

Figure 12: Marcellus shale specimens after failure in Brazilian tests.

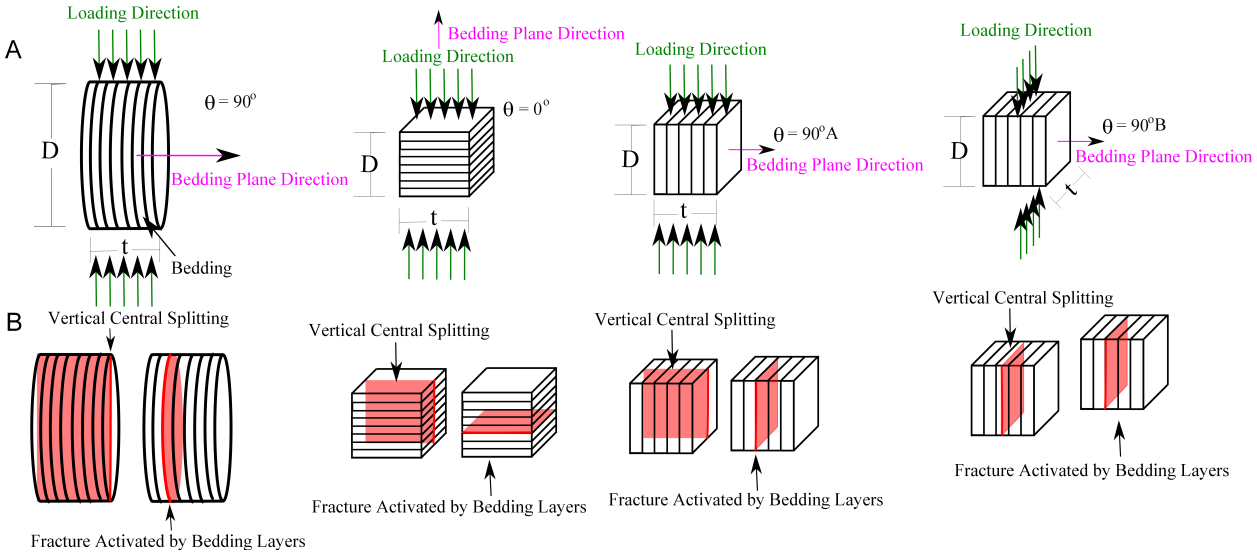

Figure 13: Brazilian tests on grey shale: (a) Loading configuration; (b) Two failure modes.

Figure 14: Grey shale specimens after failure in Brazilian tests.

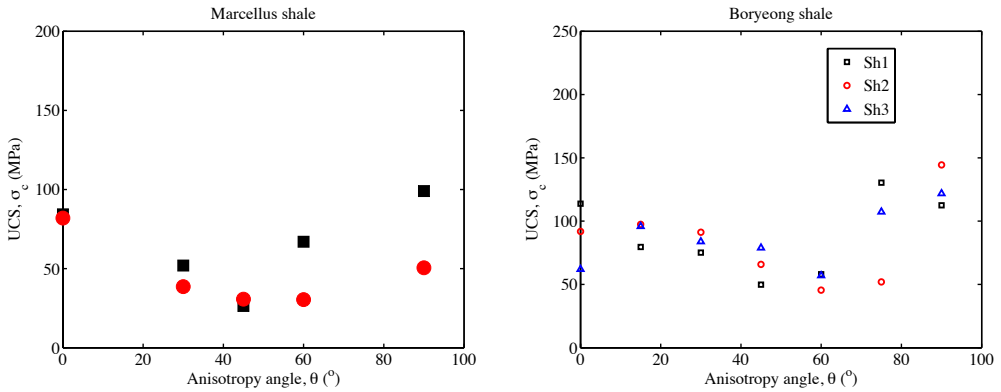

Figure 15: Compression strength variation with respect to anisotropy angle: (a) Marcellus shale; (b) Boryeong shale.

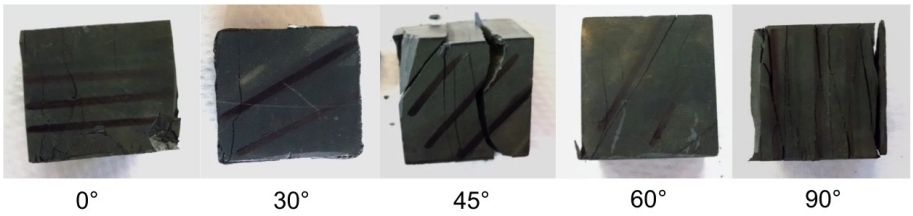

Figure 16: Marcellus shale specimens after failure in compression tests.

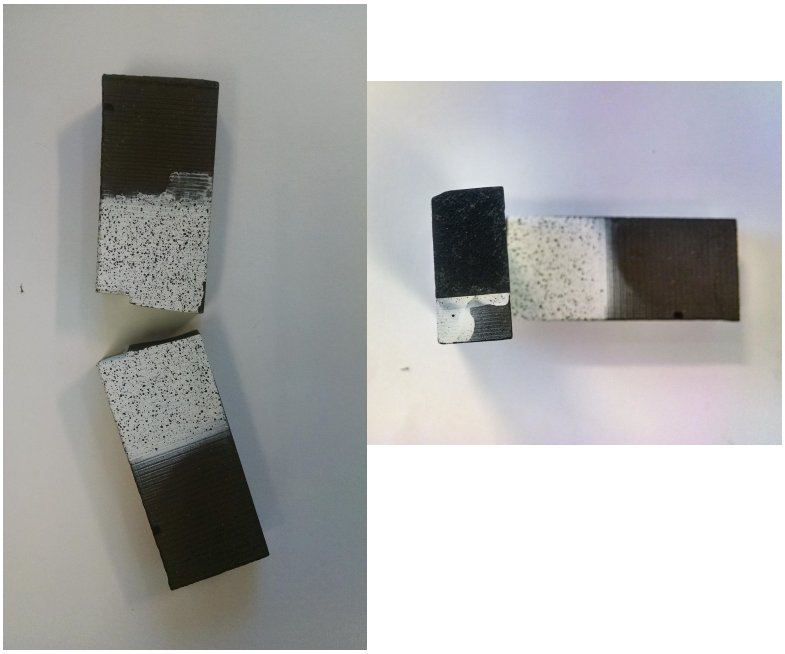

Figure 17: Marcellus shale specimens after failure in three point bending tests.